Dynamics and drivers of High Mountain Asia's glacier change from the mid 1980s to late 2019

David Loibl, Georgy Ayzel, Fiona Clubb, Inge Grünberg, Jan Nitzbon

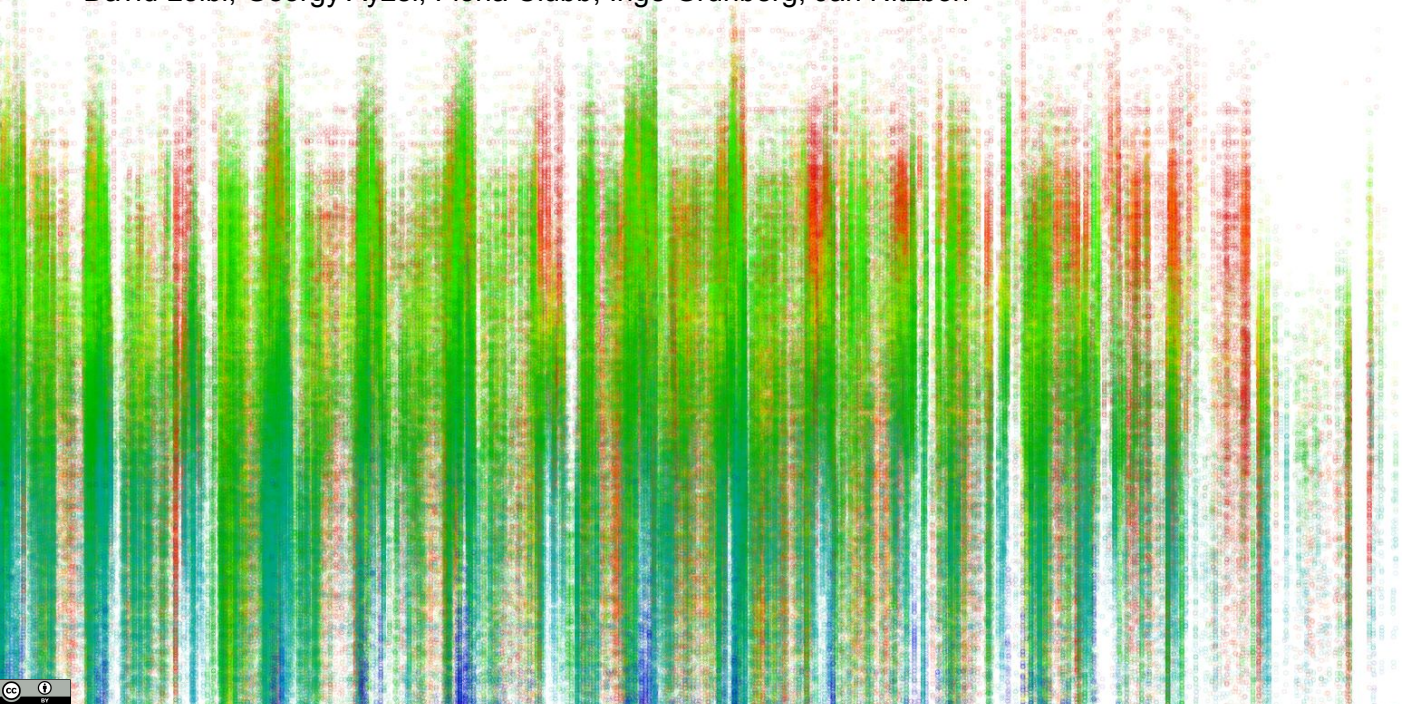

Motivation

Anthropogenic climate change has caused significant impact on glaciers across High Mountain Asia (HMA) over the past few decades. However, these effects are not spatially uniform, with glaciers throughout the region displaying heterogeneous dynamics.

Although these dynamics have been investigated by numerous studies, the drivers behind these differing responses are still poorly understood.

This is partly due to the lack of a spatially and temporally explicit dataset on glacier dynamics that has both a high spatial and temporal resolution and large spatial and temporal coverage.

Transient Snowline Altitude (TSLA)

In accordance with Østrem (1974), we use the term ‘Transient Snowline’ (TSL) to refer to the boundary between snow-covered and snow-free parts of a glacier at a specific time (. The ‘Transient Snowline Altitude’ (TSLA) is the average elevation of the TSL on a specific glacier at a specific time.

Spectral and structural contrasts facilitate TSL detection in remote sensing data, e.g. multispectral (e.g. Spieß et al., 2016, Racoviteanu et al., 2020) or SAR (e.g. Lund et al., 2020). Subsequently, digital elevation models (DEMs) can be used to obtain TSLA values.

TSLAs at the end of the melting season are a proxy for the Equilibrium Line Altitude (ELA), i.e. the elevation zone where accumulation equals ablation over a 1-year period, providing valuable indicators e.g. for mass balances and accumulation-area-ratios (e.g. Mernild et al., 2013).

→ To date, most studies aim to obtain the late summer maximum TSLA as ELA proxy (review in Rabatel et al., 2017).

→ However, technological challenges in detecting the actual end-of-season maximum and refreezing processes in accumulation areas (Cuffey and Paterson, 2010) obstruct automated large-scale applications.

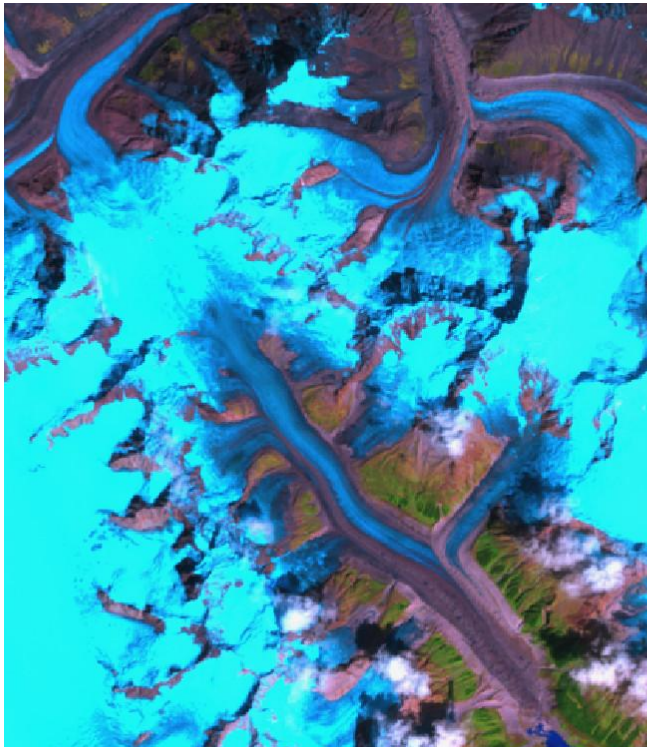

Fig. 1: Landsat ETM+ image of glaciers in southeastern Tibet in late summer (Sep 23, 1999). The false colour visualization (bands 5-4-3) shows the transient snowline as a clear contrast between light and dark blue. Note that clouds and shadows obfuscate the transient snowline locally.

TSLA measurements and postprocessing

Input data:

- Randolph Glacier Inventory v6.0 (RGI, Peffer et al., 2014)
- Landsat 5, 7 and 8 images
- ALOS World 3D 30 m DEM

Google Earth Engine processing:

- Image classification using multiple band ratio thresholds
- TSLA calculated as the median of the two lowest percentiles of the altitude range of the snow-covered part

Postprocessing (Python):

- Threshold-based filtering for situations with adverse sensing conditions, e.g. too much cloud cover, too few well-illuminated surfaces, or too few data coverage on a particular glacier.

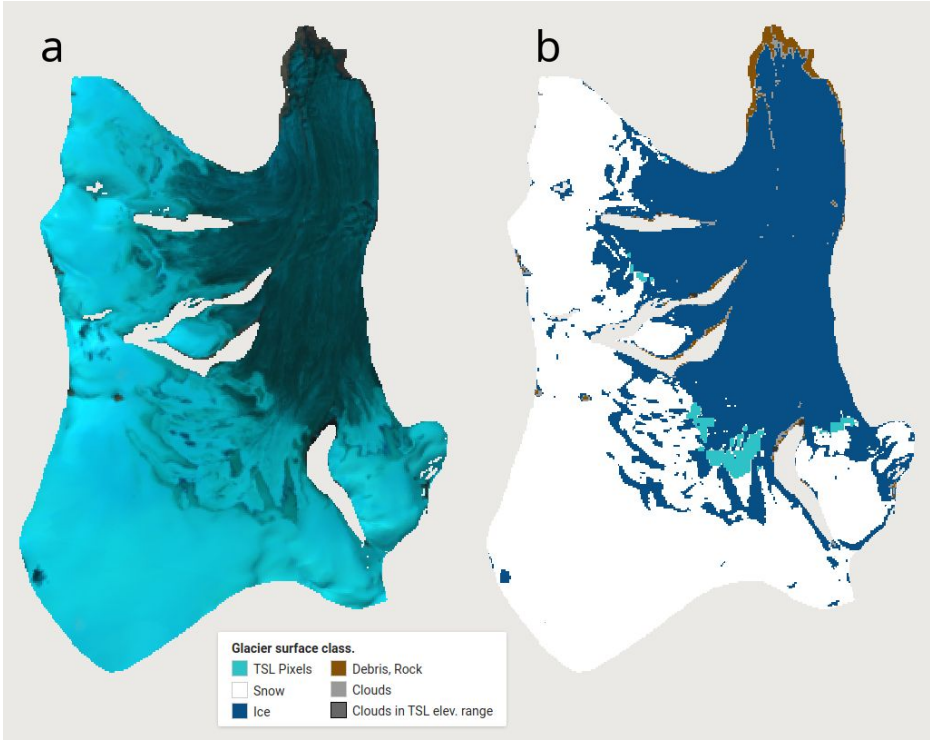

Fig. 2: Visualization of the surface material classification for a glacier in Inner Tibet (RGI60-13.53885), 2019-09-09: (a) Landsat-8 OLI image, bands 6-5-4, (b) classification result. Cyan region ('TSL Pixels') indicates the image part that is used to obtain the TSLA.

Characteristics of the TSLA dataset

Ca. 21.75 million TSLA measurements were extracted from 104,155 unique Landsat scenes. After filtering, ca. 5.94 million measurements (88,070 unique Landsat scenes) remained, forming the basis for subsequent analyses.

Latitudinal gradients and the seasonal cycle are clearly visible in the TSLA time series (Fig. 3); their patterns are inline with expectations.

Measurements per year are substantially increasing throughout the period of observation. Data gaps exist in winters 2012 and 2013.

Mean and median n obs per glacier are ca. 210 and 181, respectively.

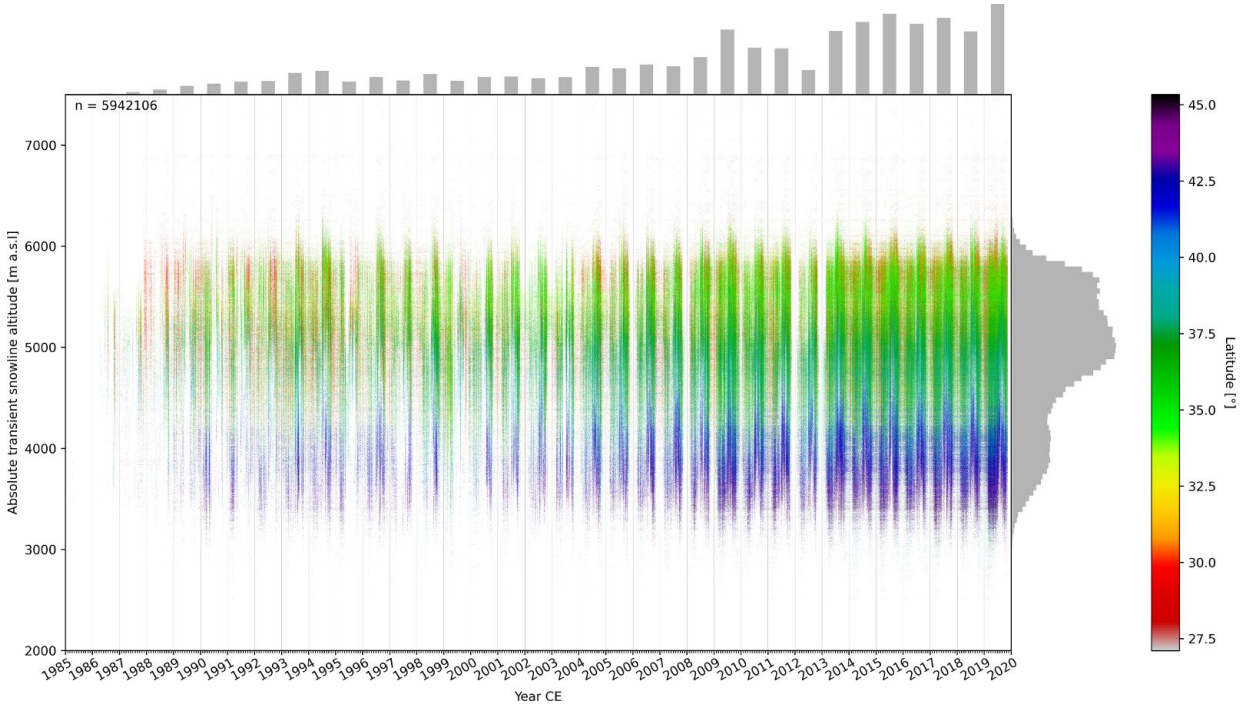

Fig. 3: TSLA measurement results for HMA and the time period 1985 to 2019, processed based on Landsat 5, 7 and 8 data in the Google Earth Engine.

The dataset was filtered for measurements overly affected by cloud cover, lacking illumination, and/or data coverage.

Characteristics of the TSLA dataset

Clear regional differences exist in the distribution of observations per glacier (Fig. 4). However, these differences are not too extreme to obstruct further analyses.

About half of the total number of glaciers (ca. 14K of 28K) have 'robust' time series with more than 100 ablation phase observations. Several glaciers with outstandingly high numbers of TSLA measurements are located in the Eastern Himalaya.

Regions with arid, continental climate regimes, such as the inner Tibetan Plateau, or the Qilian and Kun Lun Shan, exhibit the highest average time series density, presumably owing to favourable sensing conditions by prevailing clear-sky conditions.

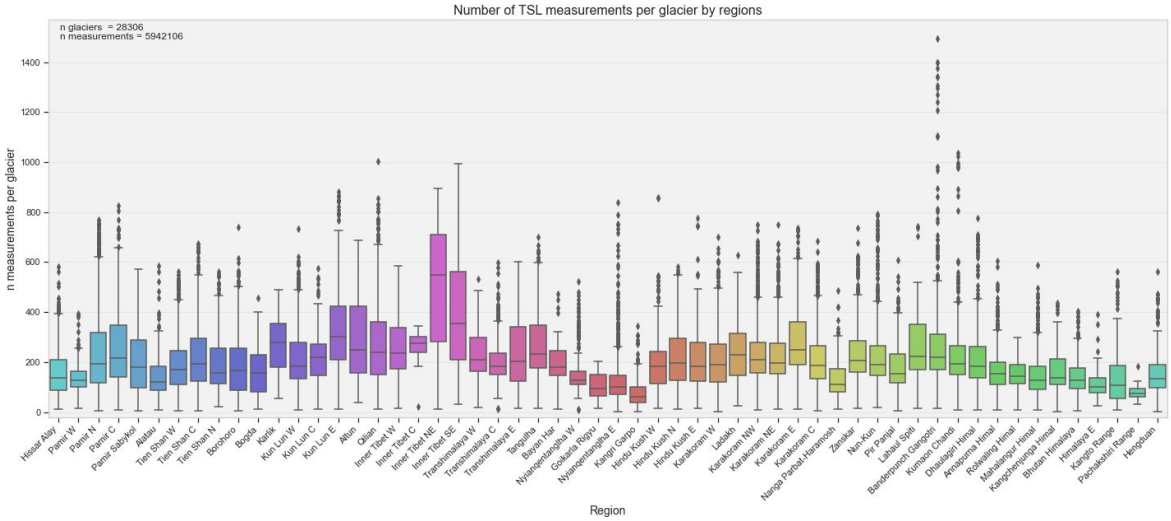

Fig. 4: Boxplots of number of observations by orographic subregions of High Mountain Asia. Ordering and colour-coding roughly resemble an Northwest (left) to Southeast (right) gradient.

Conversely, the sparsest time series are located in regions with temperate, humid climates, i.e. the monsoon-affected mountain ranges in S and E Tibet, and the Hissar Alay / Western Pamir region where advective moisture from the Westerlies meets the mountain front.

Characteristics of the TSLA dataset

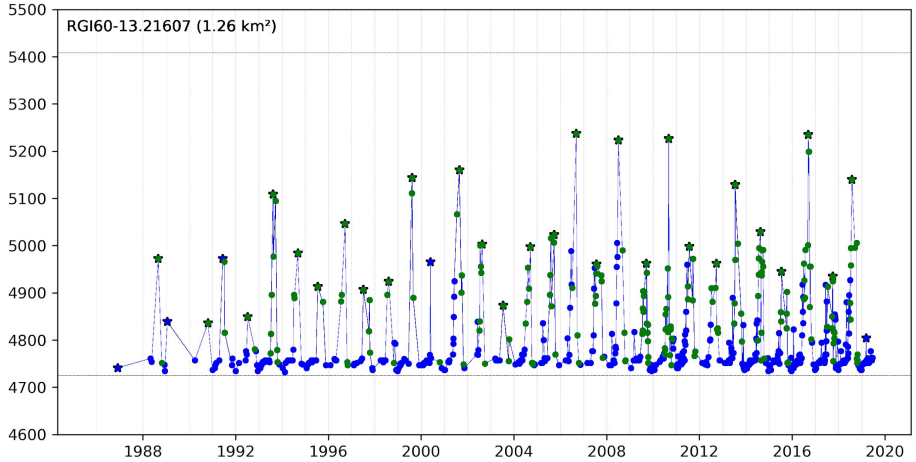

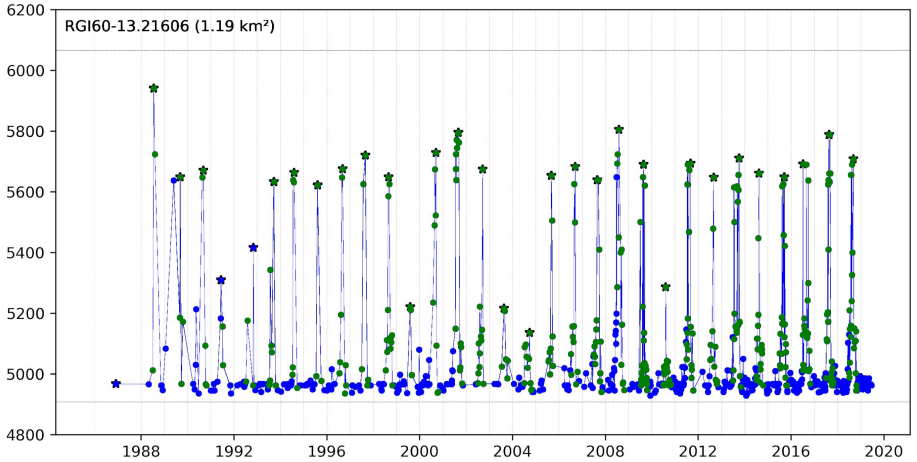

After a sufficient density of measurements is reached (typically in the early 1990s), most time series at individual glaciers clearly show the seasonal signal (Fig. 5).

However, the examples also indicate that annual maxima are frequently under- and sometimes overestimated.

Individual visual checks showed that underestimation is in almost all cases related to cloud cover during the end of the ablation season. Overestimation is a consequence of individual misclassifications that typically stem from adverse constellation of clouds, shadows, spectral characteristics of individual Landsat scenes, etc.

Fig. 5: Examples of TSLA time series for individual glaciers. Green dots indicate core ablation phase (JJAS) measurements, stars the maximum value of the respective year. Grey bars show the minimum and maximum elevation of the respective glacier.

Annual maxima and trends

Caution: Annual maxima obtained from this dataset (and arguably from most other TSL measurements, too) are highly sensitive to outliers that may have adverse effects. !

Individual glacier's total maxima of end-of-season TSLAs for the whole period of observation clearly highlight years with many (i.e. 1994, 2009, 2013, 2015) and few (i.e. 1995, 2003, 2012) maxima (Fig. 6a). The overall distribution shows a clear positive trend but also closely resembles the number of measurements per year (Fig. 3).

Only 2319 out of 28,104 glaciers exhibit trends that are significant at 0.05 level (Fig. 6b). Out of these glaciers, 78.6% have a positive trend with a median TSLA rise of 8.7 m/year.

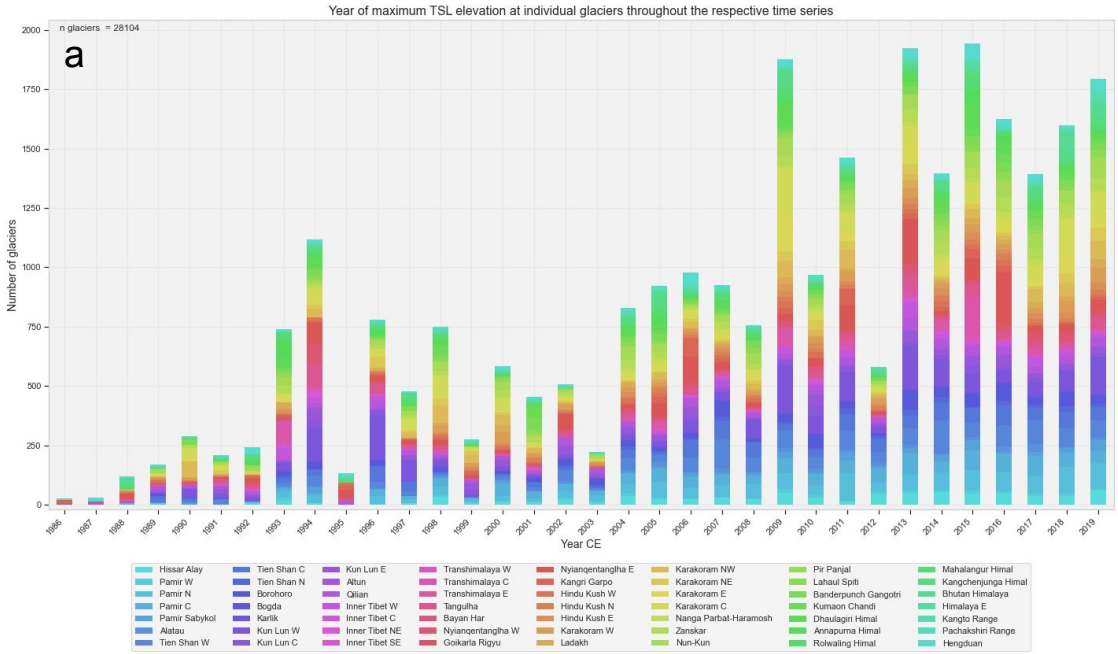

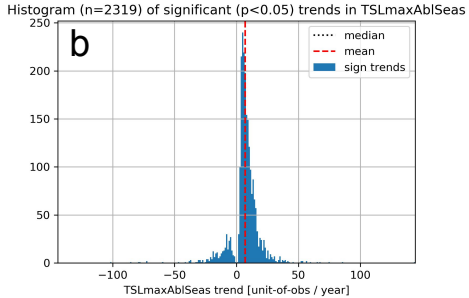

Fig. 6: Analysis of maxima in TSLA dataset: (a) Year in which the highest TSLA in the full at individual glaciers, (b) histogram of significant trends in end-of-season TSLA maxima throughout the time series.

Clustering of TSLA time series

Clusters were derived by an agglomerative hierarchical algorithm (Fig. 7).

Clustering was based on similarity (Pearson Correlation) of TSLA time series normalized to glacier elevation range.

A threshold of 100 TSLA measurements was applied to ensure robustness of the time series.

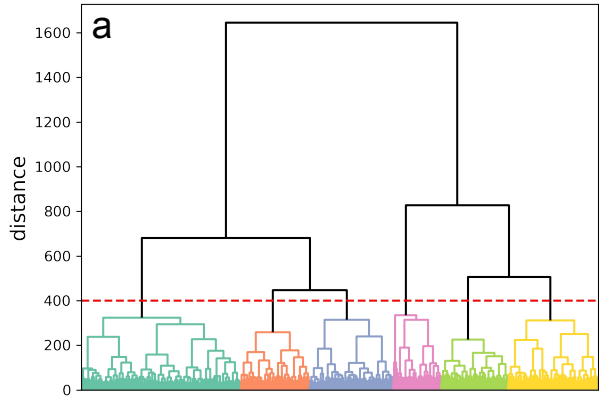

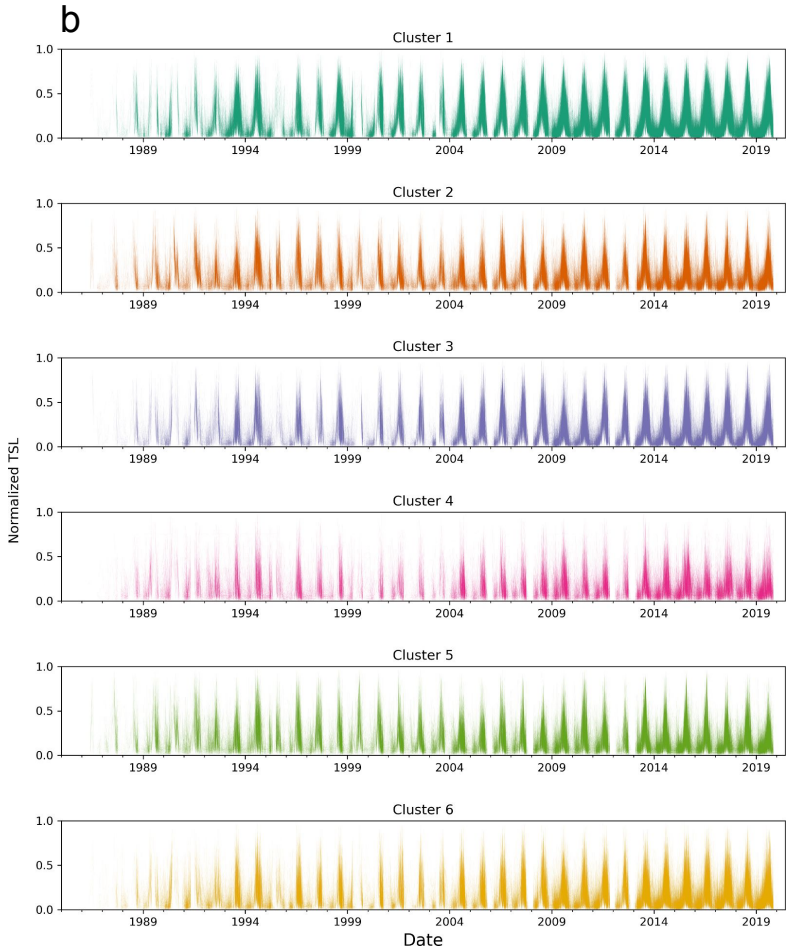

Fig. 7: Characteristics of the six clusters obtained by agglomerative hierarchical clustering: (a) Dendrogram including the dissimilarity threshold of 400, (b) normalized TSLA time series of all glaciers, grouped by clusters.

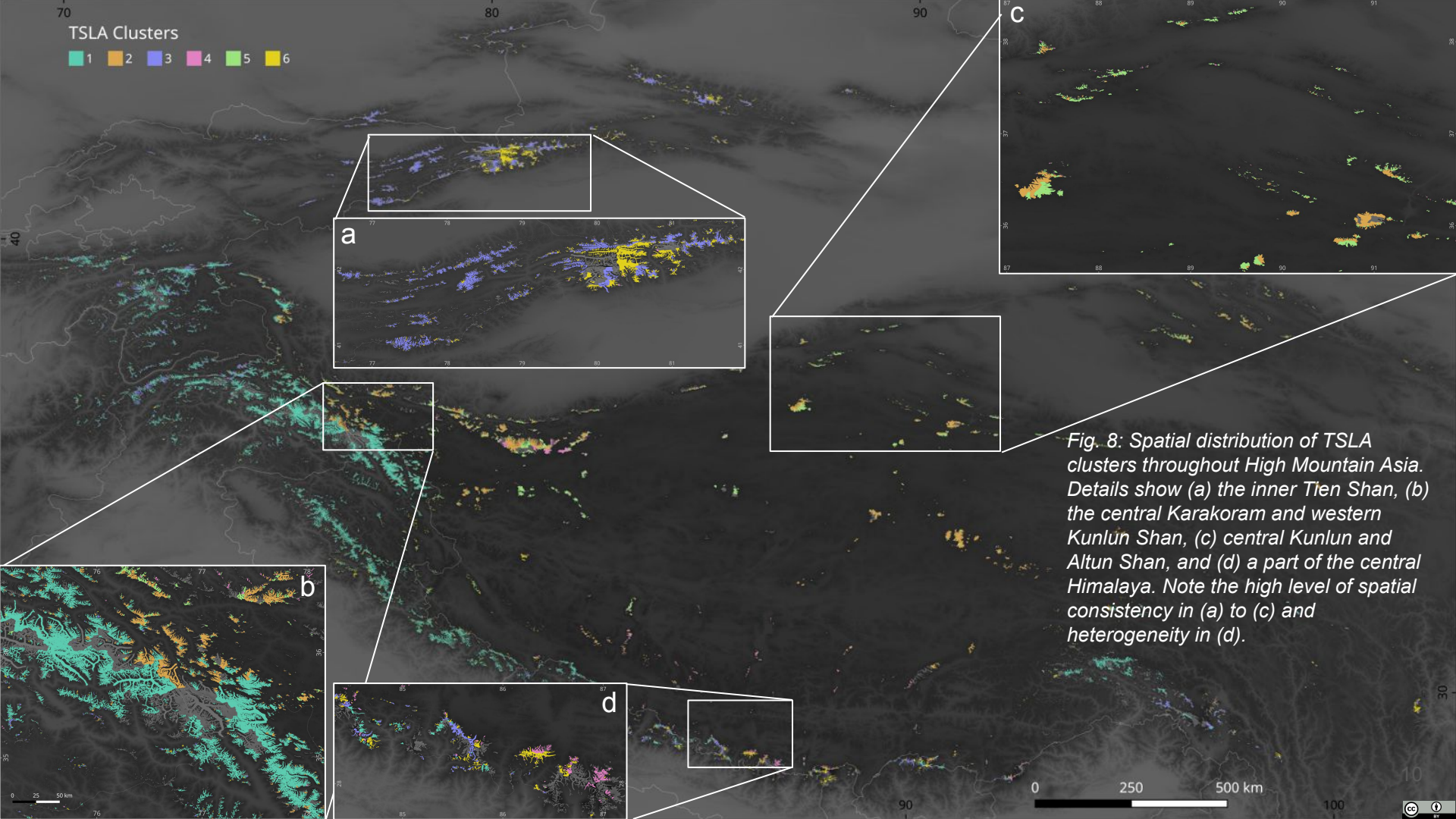

Fig. 8: Spatial distribution of TSLA clusters throughout High Mountain Asia. Details show (a) the inner Tien Shan, (b) the central Karakoram and western Kunlun Shan, (c) central Kunlun and Altun Shan, and (d) a part of the central Himalaya. Note the high level of spatial consistency in (a) to (c) and heterogeneity in (d).

Physiographic characteristics of clusters

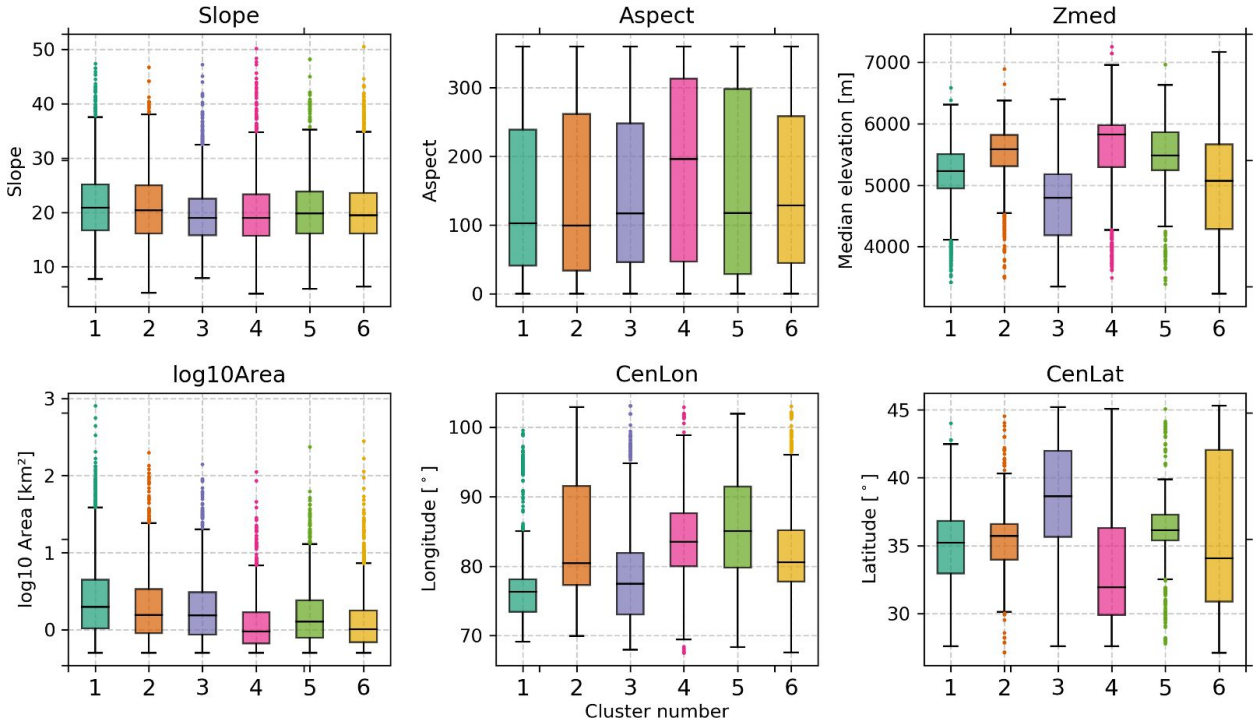

Fig. 9: Physiographic glacier characteristics by cluster. Physiographic properties for each glacier are obtained from RGI and refer to: slope angle [°], average slope aspect [°], median elevation [m a.s.l.], log base 10 of area [km²], and centroid longitude and latitude [°].

Differences in spatial location (latitude, longitude, and elevation) between clusters, despite no spatial information used in clustering algorithm.

No clear distinction in topographic metrics (slope, aspect area) between clusters. More informative topographic metrics required to understand complex forcing regimes of each glacier.

Meteorological drivers

The following meteorological parameters were extracted from ECMWF ERA5 reanalysis data and aggregated to weekly resolution:

- Temperature (2 m above ground),
- Total precipitation
- Snowfall
- Shortwave radiation downward
- Longwave radiation downward,
- Total cloud cover, and
- Wind.

Full year and core ablation phase (JJAS) were analyzed separately to investigate seasonal effects.

For each glacier, we trained a Random Forest regression model using ERA5 meteorological data as predictors for TSLA time series.

Robustness of each model was assessed using Leave-One-Out Scores.

Meteorological drivers - Cumulative for all glaciers

For the full year, temperature is clearly the dominant forcing. This is inline with expectation considering that low TSLA's are strongly correlated to low temperatures during winter.

During the core ablation season (JJAS), wind direction and snowfall become the most important drivers. This is inline with previous studies, e.g. by Mölg et al. (2012, 2017), and can be explained by the integrative role of advective regimes.

Taking a glacier in the Himalaya as an example, prevailing monsoonal influence will be coupled to a specific wind direction, presumably southern to eastern, and typically lead to relatively warm and moist conditions. Phases in which the westerlies or air masses from the Inner Plateau are advected will lead to contrasting regimes.

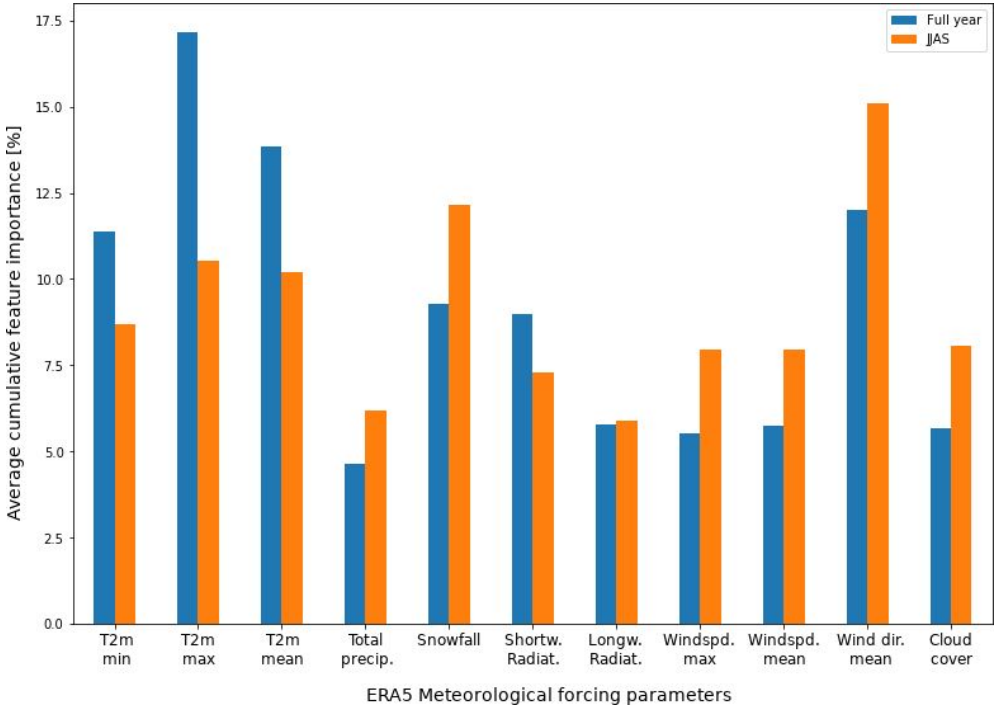

Fig. 10: Relative importances for meteorological drivers of TSLA dynamics, averaged for all Random Forest regression results. Blue bars represent data for the full year, yellow bars a subset for the core ablation season (JJAS).

Meteorological drivers - Regional averages

Regionally aggregated averages look relatively similar to each other (Fig. 11). The degree of similarity is higher than expected considering well-known regional phenomena such as the ‘Karakoram Anomaly’ (review in Farinotti et al., 2020, cf. presentation in this session) or substantial mass losses of glaciers in monsoonal SE Tibet (e.g. Wu et al., 2019).

Distributions indicate, that all meteorological factors are relevant in all regions and that differences are rather in the relative proportions.

For example, max. temperature is most important in Inner Tibet, snowfall in the western ranges, and wind direction in the central and eastern Himalayas.

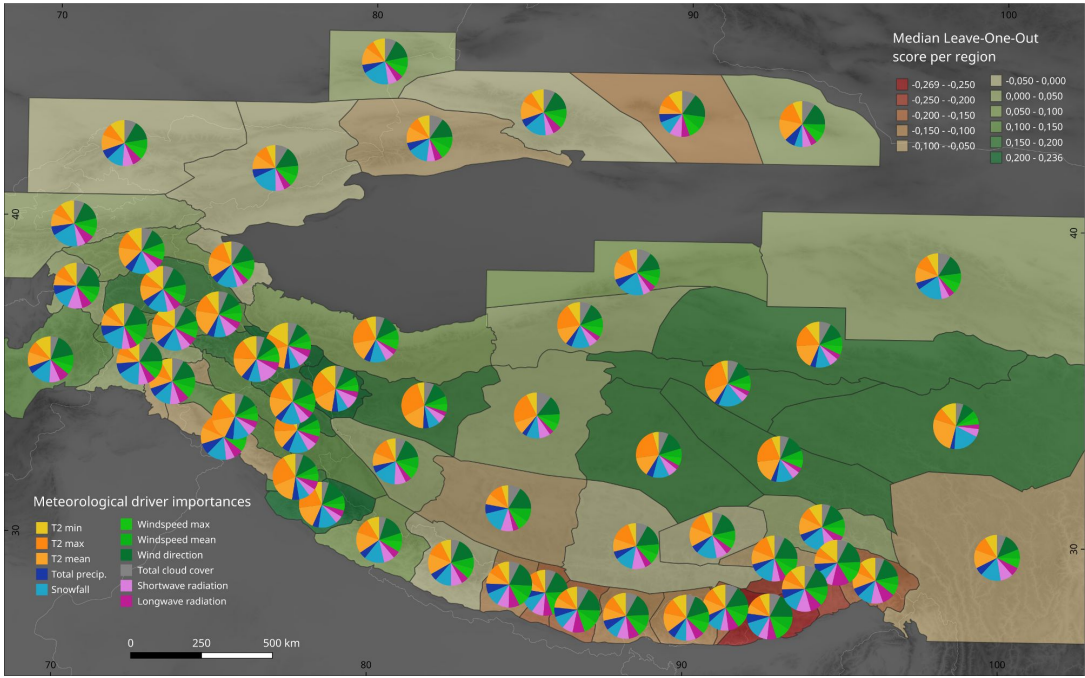

Fig. 11: Regionally averaged meteorological driver importances in the forcing of glaciers. Median leave-one-out scores provide a measure of robustness for individual regions (higher score = more robust). Contributions of drivers from individual glaciers to regional averages was scaled by individual leave-one-scores, so that only scores > 0.5 were fully considered and the impact of scores < 0 was reduced to max. 10%.

Meteorological drivers in detail

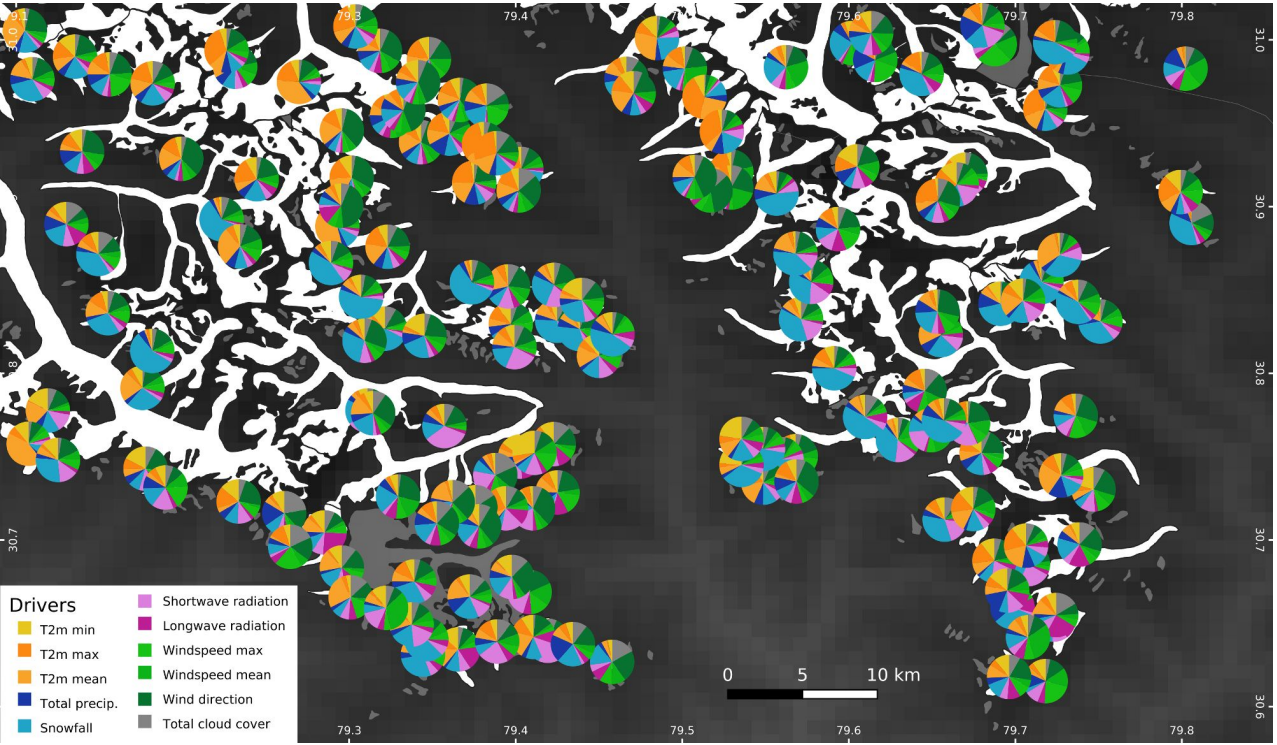

Fig. 12: Detail map of meteorological drivers obtained by Random Forest regression, taking the West Garhwal region in the eastern Himalaya as example (the large glacier in the western part of the image is Gangotri). White glacier shapes (source: RGI) represent glaciers with TSLA and driver results, grey shapes indicate one or both are not available.

At the scale of individual glaciers (Fig. 12), driver regimes exhibit (i) clear spatial patterns and (ii) substantial heterogeneity, even with adjacent glaciers.

(i) The example from the eastern Himalaya shows dominating drivers vary, i.e. temperature in the northern central part, snowfall in a band in the middle of the image, and wind direction in the southern central part.

(ii) Even though some models may not be sufficiently robust, the total picture is consistent and far from random. We have to consider heterogeneity down to the scale of individual glaciers.

Conclusions

- The TSLA dataset allows for analysing dynamics and drivers of glacier change with both high level of detail and large spatial as well as temporal coverage.

- Metrics based on annual TSLA maxima are highly sensitive to outliers which may easily occur due to adverse sensing conditions or individual misclassifications. Results of such metrics must be treated with caution.

- Conversely, metrics considering full time series, such as agglomerative hierarchical clustering and random forest regression, are more robust here. Their results based on TSLA data are widely consistent with the literature and provide detailed insights into spatial patterns and driver regimes.

- Owing to HMA's extremely complex regional to local topoclimatic systems, dynamics and drivers are often heterogeneous even for neighboring glaciers
  → Large-scale integrations may be inadequate in many cases
  → Upscaling/interpolating measurements from individual glaciers to entire HMA is rendered highly questionable

- Shortcomings in meteorological reanalysis datasets, particularly regarding precipitation, pose a major challenge in disentangling drivers. Updated and complete time series of physically-based (e.g. WRF, Maussion et al., 2014) data would be of outstanding value.

References

Cuffey, K. M. and Paterson, W. S. B.: The Physics of Glaciers, 4th ed., Butterworth Heinemann, Burlington, 2010.

Lund, J., Forster, R. R., Rupper, S. B., Deeb, E. J., Marshall, H. P., Hashmi, M. Z. and Burgess, E.: Mapping Snowmelt Progression in the Upper Indus Basin With Synthetic Aperture Radar, Front. Earth Sci., 7, doi:10.3389/feart.2019.00318, 2020.

Maussion, F., Scherer, D., Mölg, T., Collier, E., Curio, J. and Finkelnburg, R.: Precipitation seasonality and variability over the Tibetan Plateau as resolved by the High Asia Reanalysis, Journal of Climate, 27(5), 1910–1927, doi:10.1175/JCLI-D-13-00282.1, 2014.

Mernild, S. H., Pelto, M., Malmros, J. K., Yde, J. C., Knudsen, N. T. and Hanna, E.: Identification of snow ablation rate, ELA, AAR and net mass balance using transient snowline variations on two Arctic glaciers, Journal of Glaciology, 59(216), 649–659, doi:10.3189/2013JoG12J221, 2013.

Mölg, T., Maussion, F., Yang, W. and Scherer, D.: The footprint of Asian monsoon dynamics in the mass and energy balance of a Tibetan glacier, The Cryosphere, 6(6), 1445–1461, doi:10.5194/tc-6-1445-2012, 2012.

Mölg, T., Maussion, F., Collier, E., Chiang, J. C. H. and Scherer, D.: Prominent Midlatitude Circulation Signature in High Asia's Surface Climate During Monsoon, Journal of Geophysical Research: Atmospheres, 122(23), 12,702-12,712, doi:10.1002/2017JD027414, 2017.

Østrem, G.: The Transient Snowline and Glacier Mass Balance in Southern British Columbia and Alberta, Canada, Geografiska Annaler. Series A, Physical Geography, 55(2), 93–106, doi:10.2307/520877, 1973.

Pfeffer, W. T., Arendt, A. A., Bliss, A., Bolch, T., Cogley, J. G., Gardner, A. S., Hagen, J.-O., Hock, R., Kaser, G., Kienholz, C., Miles, E. S., Moholdt, G., Mölg, N., Paul, F., Radić, V., Rastner, P., Raup, B. H., Rich, J. and Sharp, M. J.: The Randolph Glacier Inventory: a globally complete inventory of glaciers, Journal of Glaciology, 60(221), 537–552, doi:10.3189/2014JoG13J176, 2014.

Rabatel, A., Sirguey, P., Drolon, V., Maisongrande, P., Arnaud, Y., Berthier, E., Davaze, L., Dedieu, J.-P. and Dumont, M.: Annual and Seasonal Glacier-Wide Surface Mass Balance Quantified from Changes in Glacier Surface State: A Review on Existing Methods Using Optical Satellite Imagery, Remote Sensing, 9(5), 507, doi:10.3390/rs9050507, 2017.

Racoviteanu, A. E., Rittger, K. and Armstrong, R.: An Automated Approach for Estimating Snowline Altitudes in the Karakoram and Eastern Himalaya From Remote Sensing, Front. Earth Sci., 7, doi:10.3389/feart.2019.00220, 2019.

Spieß, M., Schneider, C. and Maussion, F.: MODIS-derived interannual variability of the equilibrium-line altitude across the Tibetan Plateau, Annals of Glaciology, 57(71), 140–154, doi:10.3189/2016AoG71A014, 2016.

Wu, K., Liu, S., Jiang, Z., Xu, J. and Wei, J.: Glacier mass balance over the central Nyainqentanglha Range during recent decades derived from remote-sensing data, Journal of Glaciology, 65(251), 422–439, doi:10.1017/jog.2019.20, 2019.